

Study on Propagation Characteristics of the Shock Waves Driven by Gaseous Detonation Waves

Shinpei Kato¹, Satoru Hashimoto¹, Akane Uemichi¹, Jiro Kasahara¹, Akiko Matsuo²

¹Department of Engineering Mechanics and Energy,

University of Tsukuba, Ibaraki 305-8573, Japan

²Department of Mechanical Engineering, Keio University, Kanagawa 223-8522, Japan

1 Introduction

We experimentally investigated propagation characteristics of the shock wave driven by a gaseous detonation wave. In general, shock waves are considered to be generated by solid explosives or shock tubes. Although solid explosives are possible to generate shock waves even in unconfined space, it can not generate repeatedly. And, although shock tubes are relatively easy-to-use, it is also not capable of generating shock waves repeatedly. In the present research, we generate shock waves repeatedly in free space using the technology for gaseous detonation wave which is one of combustion waves and propagates at from 2 to 3 km/s. Generally, a gaseous detonation wave can be generated with a cylindrical tube filled with combustible gas, where one side is closed and the other side is open. The detonation wave begins to propagate from the closed end to the open end right after high-energy ignition. The detonation wave diffracts at the open end, and burned-pressurized gas as a piston pushes atmospheric air and creates a shock wave. Moreover, it has become possible to operate this cycle periodically at higher frequency. These mean that we could easily create finite pressure waves repeatedly in arbitrary space and arbitrary intensity at high frequency using recent pulse detonation engine (PDE) technology. In order to utilize the shock wave, its characteristics of propagation should be investigated. As for previous studies, there has been a few investigations about propagation characteristics in far field from a source of the shock wave while there has been a lot of investigations about that especially in vicinity region of a source [1, 2]. In the present study, we carried out optical visualization in vicinity region of the end of detonation tube. In far field (200 m far from the end of the tubes), we conducted fixed-point observations using piezo pressure transducers in order to obtain overpressure time-histories of the shock and pressure waves in the axial direction of the detonation tubes.

2 Experimental details

In vicinity region of the tube end, we set shadowgraph system so that we could observe around the end of a tube, where the axial of a detonation tube crossed the optical axis of shadowgraph system. In these near-field experiments, we used the detonation tube which had 25.5 mm inner diameter, 1200 mm length, and automotive spark plug (NGK D8HA) at the closed end of the detonation tube (Tube A).

The Mylar diaphragm of 12- μm thickness was used in order to separate combustible mixture inside the tube and atmospheric air out of the tube. The combustible mixture was $\text{C}_2\text{H}_4 + 3\text{O}_2$ which had been pre-mixed and we provided enough time for diffusive mixing. The detonation tube was initially filled with the combustible mixture at 1 atm. For the optical visualization, the high-speed video camera used was Hyper Vision HPV-1 (SHIMADZU Co., Ltd.) of which minimum interframe is 1 μs (the minimum exposure time: 250 ns). We carried out the near-field experiments three times and we varied observed region in each experiment. The observed regions were 15-77, 118-188, and 379-449 mm in the axial direction from the end of the tube.

In the far field from the tube end, we carried out the experiments at 1, 10, 20, 30, 98.5, and 201 m from the tube end to obtain overpressure histories of the shock and pressure waves. In a series of far-field experiments, we basically used the detonation tube which had 50 mm inner diameter and 1200 mm length (Tube B). Although, note that we carried out experiments using two different type of the tube (Tube A, Tube B) only at 1, 10 m as comparative experiments. As for the experiments at 20, 30, 98.5, 201 m, only Tube B was used. The other conditions such as the thickness of the Mylar diaphragm used, combustible mixture, spark plug, and initially filled pressure were same with those in the near-field experiments.

In addition, we also carried out another experiment independently in order to investigate the effects quantitatively which our environmental circumstances have on overpressure histories such as the reflected waves from ground surface. In its experiments, we varied the heights both of the tube h_1 and pressure transducer h_2 so that the incident shock wave and reflected shock wave had the difference of pathway distance and arrival time, resulting in separating the incident shock wave and the reflected shock wave. The conditions of each experiment were $h_1 = 0.5$ m, $h_2 = 1.0$ m where the difference of pathway distance is smaller, $h_1 = h_2 = 1.0$ m where it is larger, and $h_1 = 0.79$ m, $h_2 = 6.15$ m where it is significantly larger.

3 Parameters of the Shock wave

For obtained results, we normalized the overpressure and the axial distance from the tube end. Normalized overpressure is $P = (p - p_0) / p_0$, where p and p_0 denote absolute pressure of the shock wave and the ambient air pressure respectively. Normalized distance is $R = r/W$, where r is the distance in axial direction of the tube and W is the characteristic explosion length given by $W = \sqrt[3]{(E_0 / p_0)}$ in spherical symmetry condition. E_0 denotes the energy supplied to outside volume and we employed

$$E_0 = \frac{\pi}{3.47} p \frac{u}{a} d^3$$

[1], where d is inner diameter of the tube and p , u , a denote the absolute pressure, the particle velocity and the sound speed at Chapman-Jouguet state respectively, which were computed by Thermochemical Database of Gases and Condensed Materials : AISTJAN [6].

4 Results and Discussion

In Figure 1, the photographs are shadowgraph sequential images recorded at $t=4, 16, 28, 46$ μs , where the rupture of diaphragm are taken as $t=0$. These images are of color reversal for convenience so that originally white portion is black pattern and originally black portion is white pattern. As shown in Figure 1, the planer detonation wave gradually diffracting from the tube end and the buned-pressured gas behind the detonation wave compresses the ambient air, creating the shock wave. Additionally, we can also obtain overpressure from the observed propagation speed of the shock wave using Rankine-

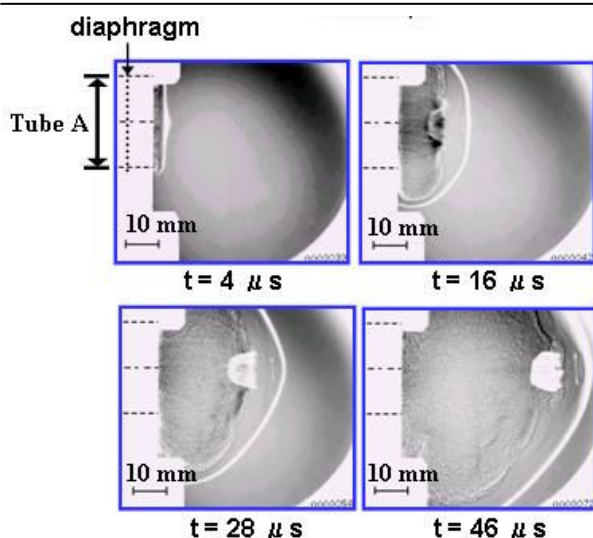
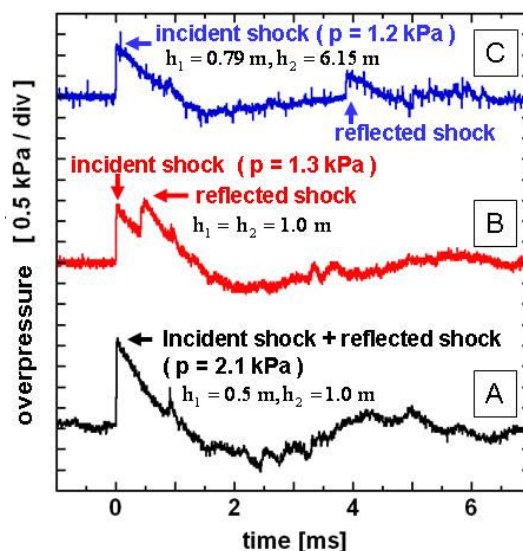


Fig.1 Shadowgraph photographs

Fig.2 The experiments varied the heights both of the tube (h_1) and the pressure gauge (h_2)

Hugoniot relations. Note that the whitish objects at center of the images in Figure 1 are considered to be the ruptured diaphragm. Figure 2-A shows time-history of the overpressure measured at 10 m from the end of the Tube B. We can observe the shock wave, the expansion wave and the negative region in pressure as shown in Figure 2-A. Similar wave form as Figure 2-A was obtained in the measurements not only at 10 m but also at 1, 20, 30, 98, 201 m. We note that the some results carried out near ground surface in the far-field experiments contain the effect of reflected wave from ground surface. Thus, we consider and eliminate the effect on the basis of our independent experiments in which we varied the heights both of the tube and the pressure transducer as mentioned previously. We show the results of it in Figure 2-A, B and C. Figure 2-A shows the shock wave which has no delayed pressure wave. In this experiment, the difference of pathway distance between incident shock wave and reflected shock wave are 0.11 m. Thus the difference of arrival time should be about 0.3 ms when we assume the speed of sound is 345 m/s. Figure 2-B shows the shock wave which has slightly delayed pressure wave and the difference of arrival time is about 1 ms. In this case, the difference of pathway distance was 0.2 ms, thus the difference of arrival time should be about 0.6 ms which is same order with the actual difference of arrival time. Figure 2-C shows the shock wave which has significantly delayed pressure wave. In this case, the difference of pathway distance was 1.0 m and the difference arrival time should be about 2.9 ms. The difference of arrival time in Figure 2-C is actually about 4 ms and same order with 2.9 ms. Thus, the delayed pressure waves in Figure 2-B and C are considered to be reflected shock wave from ground surface. This experiments show that the incident shock waves are about 57 % of the shock wave affected by the reflected wave in overpressure especially in our experimental environment. Hence, the some results were of 0.57 times in order to compare only incident shock waves each other. Now we can show the relationship between distance and the peak overpressures obtained from the near-field experiments as well as the far-field experiments. In Figure 3, we show the relationship between the normalized overpressure and the normalized distance. We can observe that the vicinity region is affected by the burned gas and consequently attenuation of the shock wave is relatively small. Right after the shock wave gets out of the vicinity region, the shock wave begins to attenuate rapidly. Subsequently, the shock wave becomes weaker and begins to have the characteristics of acoustic wave that the attenuation is proportional to $1/r$. In addition, we compare our result and previous results by Socket et al [1]. Their experiments were carried out using $H_2 + 0.5O_2$, $C_3H_8 + 3O_2$, $C_3H_8 + 5O_2$ and $C_3H_8 + 7O_2$ varied tube diameter. As mentioned previously, we

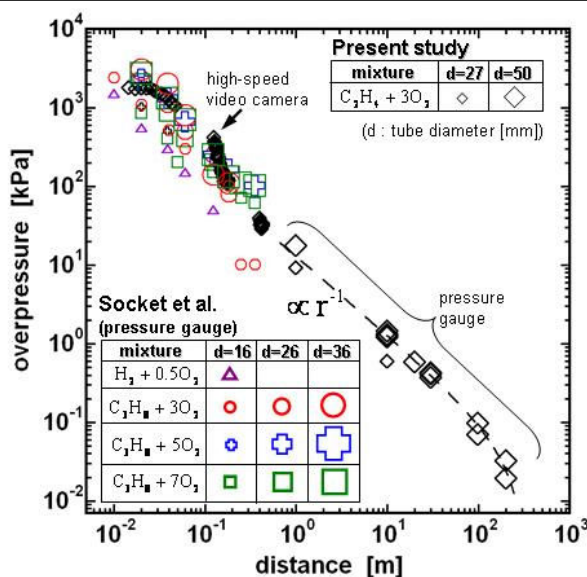


Fig.3 The relationship between axial distance and peak overpressure

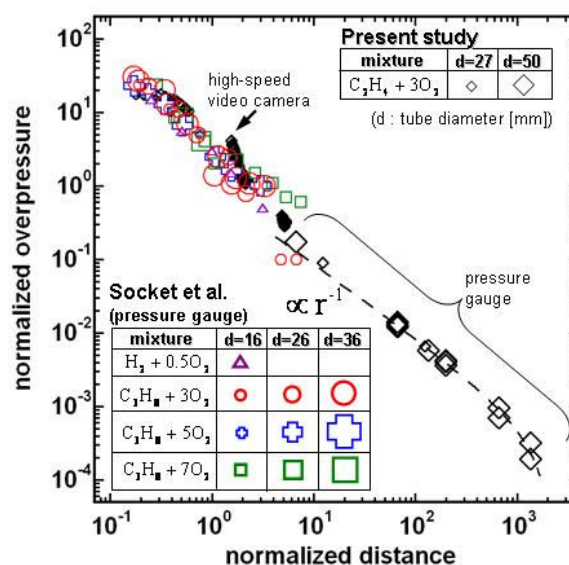


Fig.4 The relationship between normalized axial distance and normalized peak overpressure

normalize these results and show in Figure 4. Our results normalized are consistent with the results by Sochet et al. And our results obtained using different tube diameter are also well-organized by these nondimensional parameters. This result shows that the pressure waves driven by gas-detonation are able to reach 2×10^3 in normalized distance.

References

- [1] I. Sochet, T. Lamy, J. Brossard. Critical tube diameter for detonation transmission and critical initiation energy of spherical detonation. *Shock Waves*. 9 : pp.113-123
- [2] S. Sénégas, C. Vaglio, J. Brossard, R. Cayzac (2000). Quasi universal blast wave behavior. *J. Phys. IV France*. 10. Pr11: pp.91-98
- [3] J. Brossard, P. Bailly, C. Desrosier, J. Renard (1988). Overpressures Imposed by a Blast Wave. *AIAA* : pp.389-400
- [4] K. Cheval, V. Vala, O. Loiseau, S. Trélat, I. Sochet. New small scale gaseous detonation data compared with Tang and Baker's blast curves : a discussion on the energy to be considered as producing the blast wave after a gaseous detonation. *ICDERS 2007*
- [5] M. J. Tang, Q. A. Baker (1999). A new set of blast curves from vapor Cloud explosion. *Process Safety Progress*. Vol.18. No.3
- [6] K. Tanaka, "AISTJAN"
<http://riodb.ibase.aist.go.jp/ChemTherm/index-E.html>.
- [7] S. Kato, S. Hashimoto, J. Kasahara, T. Kameda, K. Takahara (2008). Study on Propagation Characteristics of Shock Waves Generated by Detonation Tube. *Symposium on Shock Waves in Japan* : pp.125-128